Ultrastructure of sonic muscles of piranhas (Serrasalmidae)

Xavier Raick[1], Nicolas Thelen[2], Philippe Compère[1] and Eric Parmentier[1]

[1] Laboratory of Functional and Evolutionary Morphology, Freshwater and Oceanic Science Unit of Research, University of Liège, B6c Allée du 6 août, 4000 Liège, Belgium

[2] Laboratory of Cell and Tissue Biology, GIGA-R, University of Liège, Giga-Neurosciences, Avenue Hippocrates 15, 4000 Liège, Belgium

Corresponding author: Xavier Raick, xavier.raick@uliege.be

Keywords: *Catoprion*, *Pygocentrus*, *Pygopristis*, *Serrasalmus*, Transmission Electron Microscopy

ORCID: Xavier Raick https://orcid.org/0000-0002-1977-0289

Abstract

Within piranhas, different species are able to make sounds but not all of them rely on the same mechanism. In all species, the sound-producing muscle originates on the second vertebra, but the insertion differs. *Pygopristis* denticulata can produce two kinds of pulsed sounds emitted in trains. Its sound production mechanism is mainly based on a muscle bundle that inserts between the two first ribs. In *Catoprion mento*, the anterior part of the sonic muscle inserts directly on the swim bladder. The most derived species (*Serrasalmus* and *Pygocentrus*) make all harmonic tonal sounds. Their sonic muscles constitute a single functional unit transversally surrounding the swim bladder. This study aims to study the ultrastructure of sonic muscles in nine species from these four genera. Epaxial muscles were compared with sonic muscles, and the sonic muscles of the different species were compared between them. Results confirmed ultrastructure modifications in the sonic muscles in comparison to epaxial muscles. Fibers of the sonic muscle are thinner and possess a thicker subsarcolemmal ring housing mitochondria. In sonic muscles, myofibrils are also proportionally less abundant, and their sarcomeres are longer and thinner. Some of these differences allows to separate basal species (e.g., *Pygopristis denticulata*) from more derived species (genera *Pygocentrus* and *Serrasalmus*) and should favour observed differences in the acoustic abilities.

Introduction

Within piranhas (Serrasalmidae), carnivorous species (*Pygopristis*, *Catoprion*, *Serrasalmus* and *Pygocentrus*) are able to produce sounds using sonic muscles acting on the swim bladder (Kastberger, 1981; Markl, 1971; Mélotte, Raick, Vigouroux, & Parmentier, 2019; Mélotte, Vigouroux, Michel, & Parmentier, 2016; Millot, Vandewalle, & Parmentier, 2011; Raick, Huby, Kurchevski, Godinho, & Parmentier, 2020a, 2020b; Raick et al., 2021). In all four genera, the mechanism involves at least the second rib, whereas sonic muscles appear to be derived from the intercostal musculature. However, important differences can also be found between the sound production mechanisms (Mélotte et al., 2019; Nelson, 1961). In *Pygopristis denticulata*, the muscles associated with sound production insert obliquely between the proximal anterior face of the second rib and the posterior surface of the first rib, at half length. Moreover, a large ligament joins the first pair of ribs to the ventral face of the first vertebra (Mélotte et al., 2019). In *Catoprion mento*, the sonic mechanism involves a muscle that inserts on the second rib and directly on the swim bladder (Mélotte et al., 2019). In the genera *Serrasalmus* and *Pygocentrus*, sound producing muscles insert on an important basal plate developed on the proximal part of the second rib. Right and left sonic muscles possess a vertical orientation and both are connected by a large tendon ventrally surrounding the anterior part of the swim bladder (Kastberger, 1981; Friedrich Ladich & Bass, 2005; Nelson, 1961). In *Serrasalmus rhombeus* and *Pygocentrus nattereri*, it has been demonstrated that these sound-producing muscles are innervated by spinal nerves, confirming their hypaxial origin (Banse, Chagnaud, Huby, Parmentier, & Kéver, 2021; Bass, Gilland, & Baker, 2008; Friedrich Ladich & Bass, 2005). Moreover, ontogenetic studies in *Pygocentrus nattereri* support that these sonic muscles are skeletal muscles whose anatomy could result from delayed development that modifies the ratio of cell components. In comparison to epaxial skeletal muscles, the quantity of myofibrils is lower, the proportion of space in the sarcoplasm is higher and the sarcoplasmic reticulum is more developed in sonic muscles (Millot & Parmentier, 2014).

Pygopristis denticulata can produce two kinds of pulsed sounds that are emitted in trains (Mélotte et al., 2019). Pulses of the first sound type are produced on an irregular basis and have a frequency of ca. 90 Hz. The pulse period is less variable in the second sound type that has a dominant frequency around 185 Hz. *Catoprion mento* can produce pulsed and tonal sounds. The pulsed sound has a period corresponding to 368 ms and a frequency of 110 Hz; the tonal sound has a period of ca. 7 ms, a frequency of 130 Hz and shows harmonics. The most derived

species (genera *Pygocentrus* and *Serrasalmus*) make all harmonic tonal sounds composed of multiple continuous cycles. The pulse period varies from 6 to 11 ms and the frequency from 120 to 170 Hz. From a global point of view, it seems that the evolution of the calls in this taxon corresponds to an increase in the ability to sustain a steady emission of pulses, meaning muscles can produce multiple trains of high-speed contractions. In *Pygocentrus nattereri*, the electric stimulation of sonic muscles and simultaneous recording of vibrations of the swim bladder wall highlighted the ability of sonic muscles to contract at high speed, corresponding to the pulse rate of natural 'bark' sounds (Kastberger, 1981; Millot et al., 2011).

Histological studies perfectly confirm assumptions about fast contracting abilities. A recent study using optical microscopy showed that diameters of sonic fibres in *Catoprion mento*, *Pygopristis denticulata* and *Pygocentrus nattereri* are significantly shorter than epaxial fibres (Mélotte et al., 2019). In different vocal teleost species, this feature has been related to the ability to sustain high-speed contractions (Millot & Parmentier, 2014; L. C. Rome, Syme, Hollingworth, Lindstedt, & Baylor, 1996). Moreover, transmission electron microscopy (TEM) has been used to characterize the sound-producing muscles in *Pygocentrus nattereri* (Millot & Parmentier, 2014) and in an unidentified carnivorous piranha species (Eichelberg, 1977, 1978). According to these studies, sonic muscles had a high volume of sarcoplasmic reticulum with an important subsarcolemmal ring space containing numerous mitochondria (Eichelberg, 1977, 1978). These features can be found in typical high-speed muscles (Appelt, Shen, & Franzini-Armstrong, 1991; Boyle, Riepe, Bolen, & Parmentier, 2015; Parmentier & Diogo, 2006; Parmentier, Marucco Fuentes, Millot, Raick, & Thiry, 2021) known to develop speed but no force during contraction (L. C. Rome et al., 1999). However, fast sonic muscles can be found in numerous no-phylogenetically related species (Friedrich Ladich, 2001; Mélotte et al., 2019; Parmentier, Bouillac, Dragicevic, Dulcic, & Fine, 2010; Parmentier et al., 2021) and are the result of evolutionary convergence. For this reason, sonic muscles found in fish from different taxa show differences in their fine structure.

In Serrasalmidae, the ability to produce sounds seems to be related to the specialization of intercostal muscles that have developed high-speed contraction features. However, the sonic system and abilities could differ within the taxa. Using TEM, the aim of this study is to discover whether the different kinds of sound-producing apparatuses possess high-speed muscles with similar ultrastructural characters. The ultrastructure of the muscles was studied in nine species of four genera (*Pygopristis*, *Catoprion*, *Serrasalmus* and *Pygocentrus*). Epaxial muscles were

compared with sonic muscles, and the sonic muscles of the different species were compared between them.

Materials and Methods

Biological materials and observations

Samples of muscles were taken from each of the following species: *Catoprion mento, Pygocentrus piraya, Pygocentrus nattereri, Pygocentrus cariba, Pygopristis denticulata, Serrasalmus spilopleura, S. elongatus, S. manueli* and *S. compressus* (Standard length: 55 – 126 mm). Sex of the specimens was not determined. All the species were obtained in aquarium trades in Belgium. One specimen of each species was euthanized with an overdose of MS222 (500 mg L^{-1}). We decided to only use one specimen per species for ethical and logistic reasons. The specimens used were involved in a larger study approved by the ethical commission of the University of Liège (case 1532). However, according to national legislations, no permit was necessary for collecting the biological material. Two kinds of muscles were selected for the study: sonic muscles and epaxial muscles. Epaxial muscles are usually chosen as a control in this kind of study (Mélotte et al., 2019; Millot & Parmentier, 2014; Parmentier et al., 2021). Having the same muscles sampled in different species allows comparisons to be made.

The muscles were fixed by immersion in a solution of 2.5% glutaraldehyde in 0.1 M Na-cacodylate pH 7.4 for 24 h and then rinsed in 0.2 M cacodylate buffer. The samples were post-fixed in 1% osmium tetroxide, rinsed in MilliQ-water, then dehydrated through an ethanol-propylene oxide series and embedded in epoxy resin (SPI-PON 812, SPI-CHEM, USA). Transversal and longitudinal semithin sections (1 µm) were cut with a diamond knife mounted on a Reichert Ultracut E ultramicrotome. The semithin sections were then stained in 2% toluidine blue at pH 9.0, observed with a Leica MD 1000 binocular microscope and photographed with Leica LAS EZ software to see the general organization of the muscles. The areas of interest were ultrathin sectioned (60-80 nm) and stained with uranyl acetate and lead citrate and observed with a JEM-1400 Transmission Electron Microscope (Jeol Ltd, Tokyo, Japan) at 80 kV accelerating voltage.

Measurements

Different parameters were measured on the pictures of muscles in both transversal and longitudinal sections using Adobe Photoshop Elements 11 (Adobe Systems, San José, California) (Fig. 1) to determine the characteristics, according to Parmentier et al. (2021).

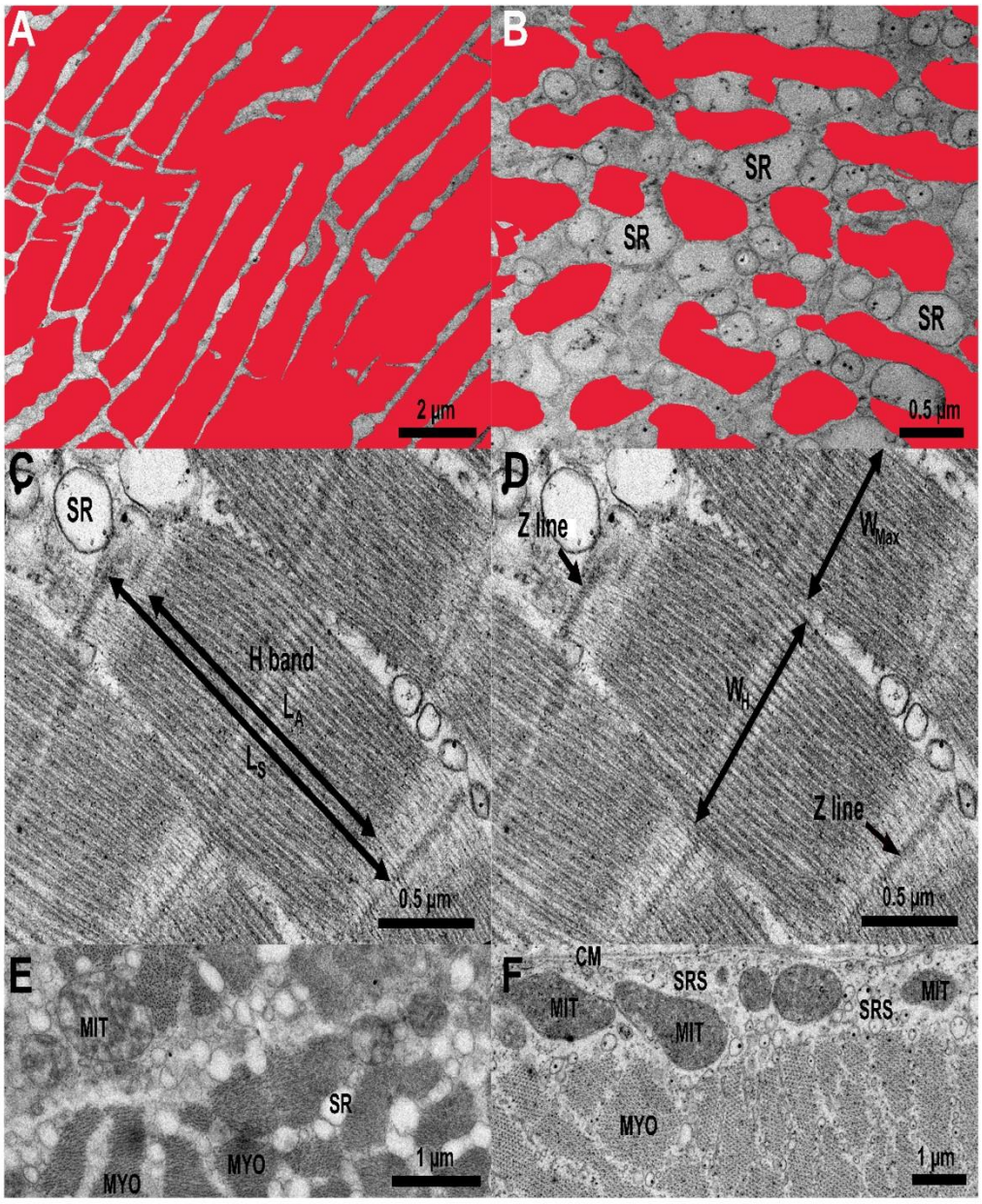

Fig. 1. Illustration of muscle structures and their measurements. **(A)** Transversal section in an epaxial muscle of *Serrasalmus spilopleura* with myofibrils coloured red to calculate the ratio of area occupied by myofibrils (**%M**). (**B)** Transversal section in a sonic muscle of *Serrasalmus spilopleura* with myofibrils highlighted in red to calculate **%M. (C)** and **(D)** Longitudinal sections in an epaxial muscle of *Pygocentrus cariba* with different measures of sarcomeres. **(E)** Transversal sections in the centre of a cell of sonic muscle of *Catoprion mento* and **(F)** Subsarcolemmal ring space of a sonic muscle cell of *Pygopristis denticulata*. SRS = Subsarcolemmal ring space. SR = Sarcoplasmic reticulum. MYO = myofibrils, MIT = mitochondrion, CM = cell membrane, L_S = Sarcomere length. L_A = A-band length. W_H = width of the sarcomere measured at the level of the H-zone. W_{Max} = maximal width of the sarcomere. DM = diameter of the myofibrils.

On longitudinal sections taken at magnification of 12 000 x, the number of sarcomeres per 10 µm^2 (**nS**, without unit) was counted on 10 pictures per cell in three different cells in each muscle of each species. The following parameters were measured on 20 sarcomeres per cell in three different cells in each muscle of each species: the sarcomere length (**LS**, in nm, Fig. 1) from the centre of a Z-line to the centre of the next one; the A-band length (**LA**, in nm) corresponding to the length of the myosin; the I-band length (**LI**, in nm) defined as $L_I = L_S - L_A$; the I-band to A-band ratio (**RIA**, without unit) defined as $R_{IA} = L_I\ L_A^{-1}$; the width of the sarcomere measured at the level of the H-zone (**WH**, in nm); the maximal width of the sarcomere (**WMax**, in nm, Fig. 1) measured anywhere in the sarcomere.

The cross-section cell area (**surface**, in µm^2) was measured on transversal sections, at different magnifications. The following parameters were measured in five different cells in each muscle of each species at 4 000 x magnification: the ratio of area occupied by myofibrils (**%M,** Fig. 1); the diameter of the myofibrils (**DM**, in nm) obtained by averaging the diameter of five myofibrils per cell; the width of the subsarcolemmal ring (**R**, in nm) obtained by averaging five measurements corresponding to the shortest distance between the sarcoplasmic membrane and the closest myofibril; the density of mitochondria in the subsarcolemmal ring (**mR**, in nm^{-2}) measured as the number of mitochondria in the subsarcolemmal ring divided by the surface of the ring; the density of mitochondria in the cell except those in the subsarcolemmal ring (**mM**, in nm^{-2}) measured as the number of mitochondria in this area (i.e., all the cell except the subsarcolemmal ring) divided by the whole area of the cell cross-section; the total density of mitochondria (**mT**, in nm^{-2}) defined as $m_T = m_R + m_M$. In addition, some cells had a central area without myofibrils. This area is called a core zone. For those cells, the size of the core zone (in nm^2) was divided by the size of the cell (in nm^2) to assess its importance (**C**, without unit).

Statistics

Statistical analyses were performed with R software 3.6 (R Core Team, 2019). Data are presented as mean ± standard deviation. A Wilcoxon-Mann-Whitney test was used to compare the sonic and the epaxial muscles, while Kruskal-Wallis followed by Dunn *post hoc* tests were used to compare the sonic muscles of the different species. In addition, the multivariate aspect of measurements on transversal sections was examined with a hierarchical clustering (Ward's method, Euclidean distance) on the standardized features measured in transversal sections of sonic muscles. A principal component analysis (PCA) on the correlation matrix was realized on the same data. Finally, a PCA on both kinds of muscle was realized to visualize them on the same graph. The link between PCs and features was calculated with a Spearman matrix of

correlation with *P*-values adjusted by the Holm method. The level of uncertainty was 0.05 for all the tests.

Results

Sonic muscles vs. *epaxial muscles*

When considering all the species together, sonic and epaxial muscles in Serrasalmidae were highly different in both size and features of their different components. Core zones were more abundant in sonic muscles, but they were always very small (maximum 2 to 3% of the cell).

In cross section, cells in sonic muscles are smaller than in epaxial muscles (**surface**: 1360 ± 979 µm^2 vs. 2464 ± 1434 µm^2; Wilcoxon-Mann-Whitney: W = 823, *P* = 0.0008, Fig. 2). The ratio of area occupied by myofibrils was lower in sonic muscles than in epaxial muscles (46 ± 12% vs. 72 ± 12%; Wilcoxon-Mann-Whitney: W = 1067, *P* < 0.0001). In addition, sonic muscles contain a higher number of sarcomeres per surface unit (4.49 ± 1.94 per 10 µm^2 vs. 3.32 ± 1.79 per 10 µm^2; Wilcoxon-Mann-Whitney: W = 16257, *P* < 0.0001). These sarcomeres are longer (for both $\mathbf{L_S}$, $\mathbf{L_A}$ and $\mathbf{L_I}$; Table 1) and thinner (both $\mathbf{W_H}$ and $\mathbf{W_{max}}$; Table 1, Fig. 3) in sonic muscles than in epaxial muscles. In both epaxial and sonic muscles, triads appear at the level of the Z-line and they possess a central vesicle that is much smaller than the two lateral terminal cisternae (Fig. 3).

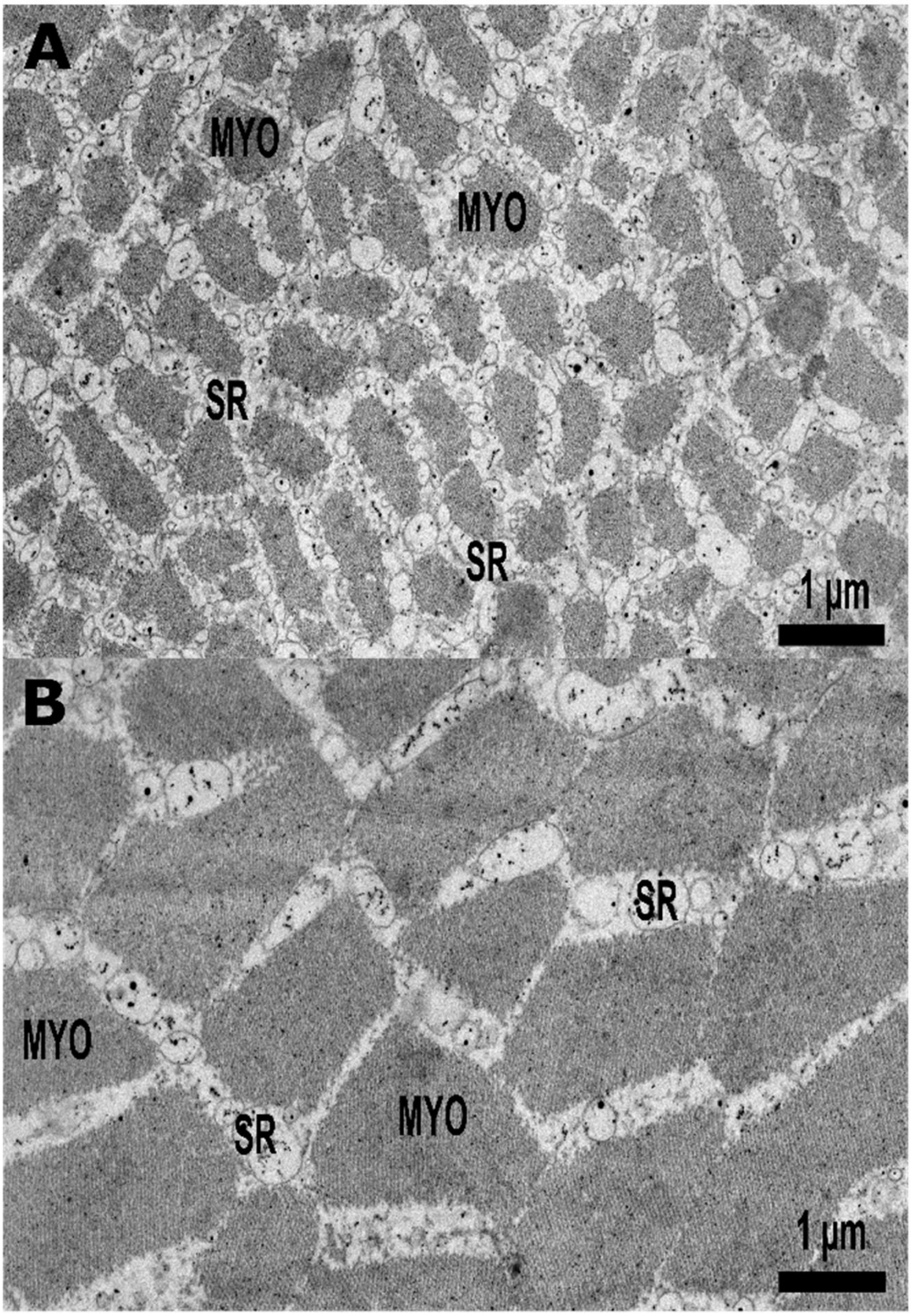

Fig. 2. TEM images of *Pygocentrus piraya* sonic **(A)** and epaxial **(B)** muscles in transversal section. SR = sarcoplasmic reticulum. MYO = myofibrils. The magnification is the same for both pictures.

Table 1 Mean, standard deviation (SD) and comparison values of each feature between epaxial and sonic muscles of all studied species. Significant values in red. Means are based on all data from all specimens. $\mathbf{n_S}$ = number of sarcomeres per 10 µm^2, $\mathbf{L_S}$ = sarcomere length, $\mathbf{L_A}$ = A-band length, $\mathbf{L_I}$ = I-band length, $\mathbf{W_H}$ = width of the sarcomere measured at the level of the H-zone, $\mathbf{W_{Max}}$ = maximal width of the sarcomere, **surface** = cross-section cell area, **%M** = ratio of area occupied by myofibrils, **DM** = diameter of the myofibrils, **R** = width of the subsarcolemmal ring, $\mathbf{m_R}$ = density of mitochondria in the subsarcolemmal ring, $\mathbf{m_M}$ = density of mitochondria in the cell except those in the subsarcolemmal ring, $\mathbf{m_T}$ = total density of mitochondria, **C** = size of the core zone divided by the size of the cell.

	Epaxial muscle		**Sonic muscle**		**Wilcoxon-Mann-Whitney test**	
	Mean	**SD**	**Mean**	**SD**	**W**	***P***
Measurements of longitudinal sections (12 000 x magnification) n = 540 except for n_S, n = 270						
$\mathbf{n_S}$	3.32	1.79	4.49	1.94	16257	< 0.0001
$\mathbf{L_S}$ (nm)	1337	569	1735	278	67859	< 0.0001
$\mathbf{L_A}$ (nm)	1150	507	1433	191	86871	< 0.0001
$\mathbf{L_I}$ (nm)	186	95	303	148	71920	< 0.0001
$\mathbf{R_{IA}}$	0.17	0.09	0.21	0.09	83683	< 0.0001
$\mathbf{W_H}$ (nm)	818	432	527	305	196167	< 0.0001
$\mathbf{W_{Max}}$ (nm)	839	443	567	326	192189	< 0.0001
Measurements of transversal sections (variable magnification) n = 45						
surface (µm^2)	2464	1434	1360	979	823	0.0008
Measurements of transversal sections (4 000 x magnification) n = 45						
%M (%)	72	12	46	12	1067	< 0.0001
DM (nm)	1027	210	429	155	1139	< 0.0001
R (nm)	572	501	2274	1550	75	< 0.0001
C (%)	0.21	0.60	0.49	0.86	404	0.15
$\mathbf{m_R}$ (nm^{-2})	$2.16\ 10^{-7}$	$3.51\ 10^{-7}$	$2.94\ 10^{-7}$	$2.45\ 10^{-7}$	339	0.02
$\mathbf{m_M}$ (nm^{-2})	$6.16\ 10^{-10}$	$6.72\ 10^{-10}$	$4.90\ 10^{-9}$	$1.16\ 10^{-8}$	422	0.08
$\mathbf{m_T}$ (nm^{-2})	$2.09\ 10^{-7}$	$3.47\ 10^{-7}$	$2.98\ 10^{-7}$	$2.50\ 10^{-7}$	344	0.01

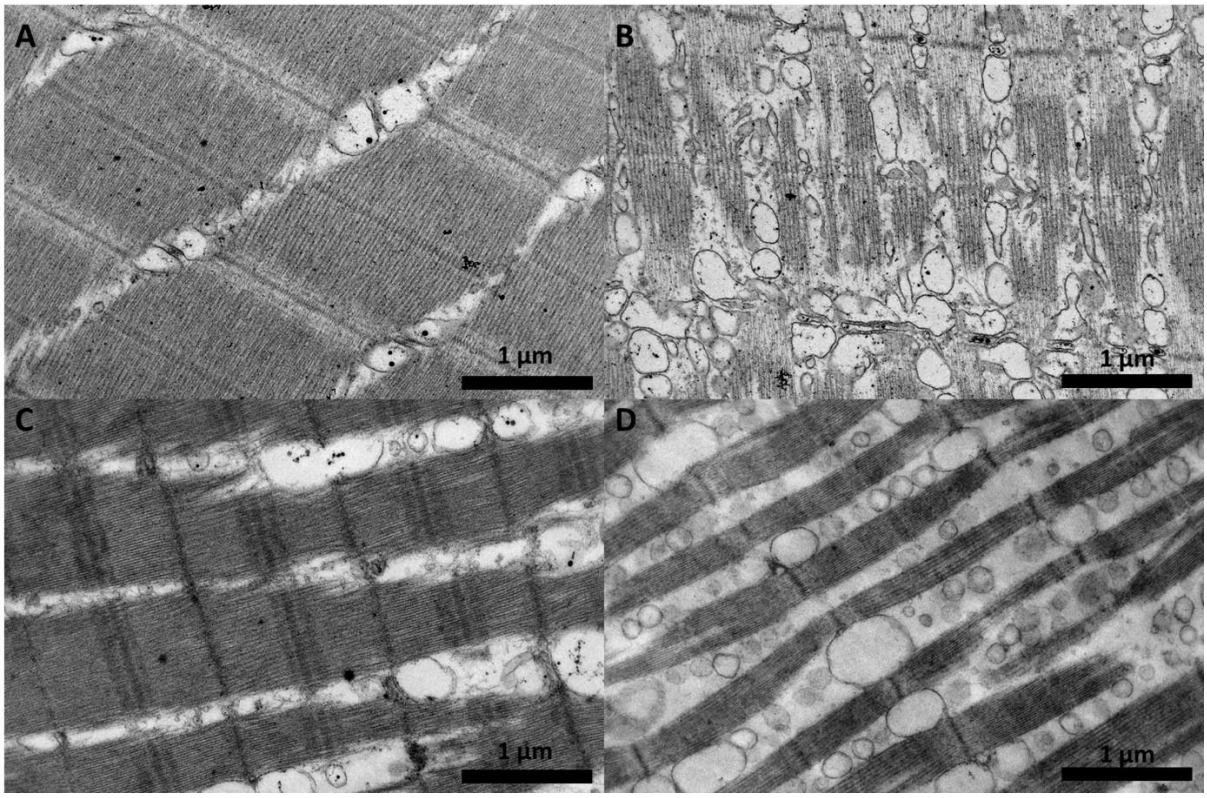

Fig. 3. TEM views of muscle longitudinal sections. **(A)** Epaxial muscle of *Pygocentrus cariba*. **(B)** Sonic muscle of *P. cariba.* **(C)** Epaxial muscle of *Serrasalmus manueli*. **(D)** Sonic muscle of *S. manueli*.

In all muscles, vesicular sarcoplasmic reticulum was found between the myofibrils (Fig. 2A and 3D). In addition, several cells had sarcoplasmic reticulum concentrated in small, dispersed patches that could be observed in the centre of the cell, but not exclusively (Fig. 1E). This situation was found in a minority of cells and did not differ statistically between sonic and epaxial muscles (Wilcoxon-Mann-Whitney: W = 404, $P = 0.15$). The subsarcolemmal ring was thicker in sonic muscles than in epaxial muscles (2274 ± 1550 nm vs. 572 ± 501 nm; Wilcoxon-Mann-Whitney: W = 75, $P < 0.0001$, Table 1) and contains a higher number of mitochondria in comparison to epaxial muscles ($2.94\ 10^{-7} \pm 2.45\ 10^{-7}$ nm^{-2} vs. $2.16\ 10^{-7} \pm 3.51\ 10^{-7}$ nm^{-2}; Wilcoxon-Mann-Whitney: W = 339, $P = 0.02$). The density of mitochondria in the cell except those in the subsarcolemmal ring ($\mathbf{m_M}$) did not differ between both types of muscle ($4.90\ 10^{-9} \pm 1.16\ 10^{-8}$ nm^{-2} vs. $6.16\ 10^{-10} \pm 6.72\ 10^{-10}$ nm^{-2}; Wilcoxon-Mann-Whitney: W = 422, $P = 0.08$). The density of mitochondria was higher in the subsarcolemmal ring than in the rest of the cell (Table 1).

The intraspecific comparison of epaxial and sound-producing muscles provided additional information supporting that all species show different ultrastructural organizations of sonic muscles. In *Pygopristis denticulata*, no significant difference appeared in the **ns**

between sonic (4.92 ± 2.04 per 10 µm^2) and epaxial muscle (5.29 ± 2.75 per 10 µm^2; Wilcoxon-Mann-Whitney: W = 432, *P* = 0.67) nor in the **DM** (637 ± 143 nm for sonic muscle and 814 ± 87 nm for epaxial muscle; Wilcoxon-Mann-Whitney: W = 22, *P* = 0.056).

Comparison of sonic muscles between species

The measured parameters of sound-producing muscle cells in each species were compared. The results revealed that cells have a smaller size in *Catoprion mento* and *Pygopristis denticulata* (335 ± 147 µm^2 and 468 ± 190 µm^2 respectively; mean **surface** ± SD) than in *Pygocentrus* species (2540 ± 321, 2208 ± 1477 and 1463 ± 619 µm^2, Fig. 4, Table 2). This difference in cell area in transversal sections was significant between *C. mento* and two *Pygocentrus* species: *P. nattereri* and *P. piraya* (Kruskal-Wallis: χ^2 = 29.82, df = 8, *P* = 0.0002; Dunn: Z = −3.08 and −4.06, *P* = 0.02 and 0.002) as well as between *P. denticulata* and the same *Pygocentrus* species (Dunn: Z = 2.68 and 3.65, *P* = 0.04 and 0.005). In *Serrasalmus* spp., the mean area of the muscle cell transversal sections was intermediate, ranging from 427 to 2033 µm^2 (Table 2). All the *Serrasalmus* species were statistically equivalent to all the *Pygocentrus* species (Dunn: all *P* > 0.05 except between *S. manueli* and *P. piraya*; Z = −2.79 and *P* = 0.03) whereas three of the four *Serrasalmus* species were statistically equivalent to both *C. mento* and *P. denticulata* (Dunn: all *P* > 0.05 except for *S. spilopleura*: Z = −3.27 and −2.87, *P* = 0.01 and 0.03).

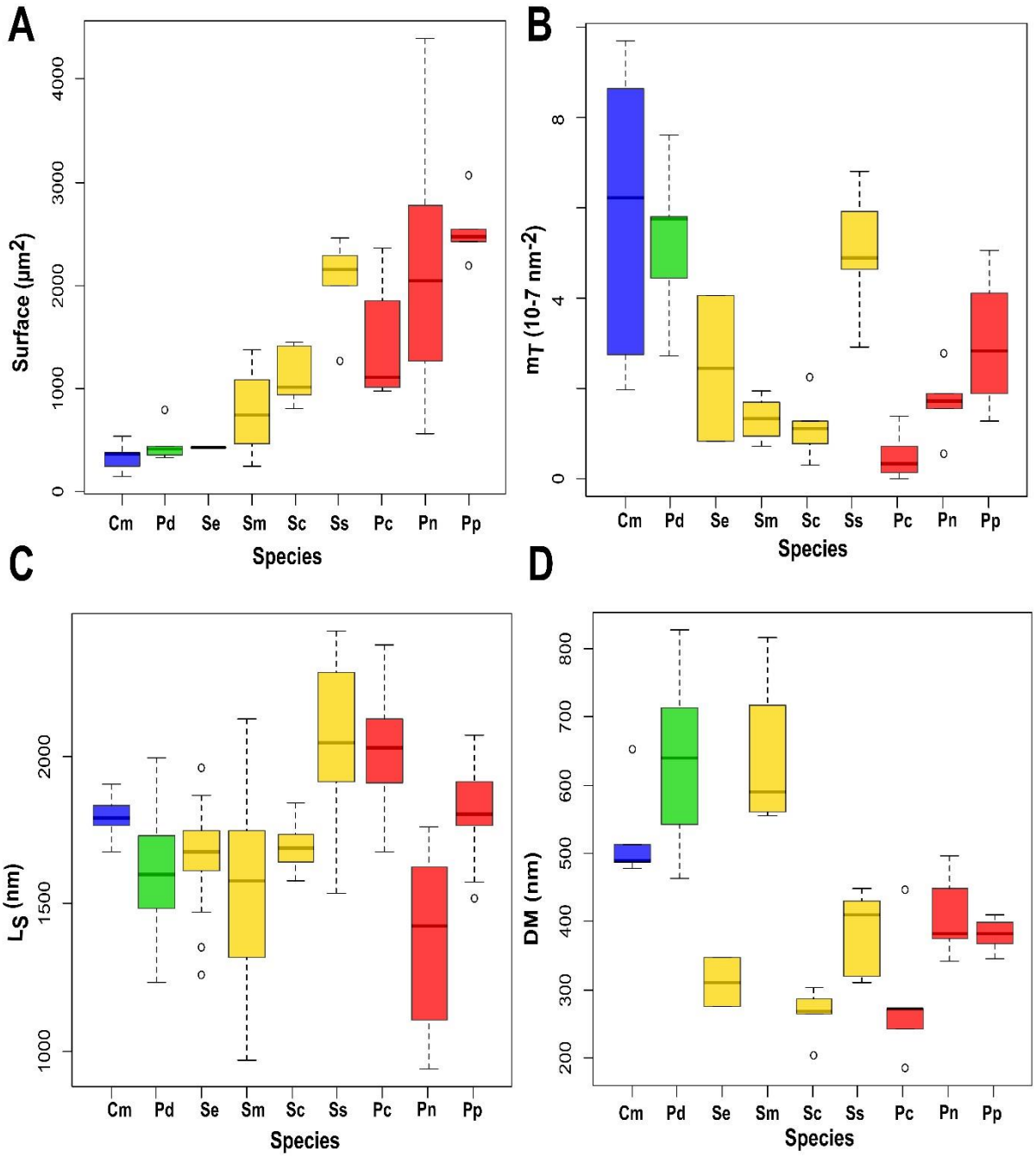

Fig. 4. Boxplots of muscle cell features in the different species. Cell surface **(A)**, total density of mitochondria **(B)**, sarcomere length (**C)** and diameter of the myofibrils **(D)**. Cm = *Catoprion mento*, Pd = *Pygopristis denticulata*, Se = *Serrasalmus elongatus*, Sm = *Serrasalmus manueli*, Sc = *Serrasalmus compressus*, Ss = *Serrasalmus spilopleura*, Pc = *Pygocentrus cariba*, Pn = *Pygocentrus nattereri* and Pp = *Pygocentrus piraya*. In blue: *Catoprion* genus, green: *Pygopristis* genus, yellow: *Serrasalmus* genus and red: *Pygocentrus* genus.

Table 2 Mean and Standard Deviation (SD) values of each feature for the sonic muscles of each studied species.

	Catoprion mento		***Pygopristis denticulata***		***Pygocentrus piraya***		***Pygocentrus nattereri***		***Pygocentrus cariba***	
	Mean	**SD**	**Mean**	**SD**	**Mean**	**SD**	**Mean**	**SD**	**Mean**	**SD**
$\mathbf{n_S}$	2.86	1.08	4.92	2.04	3.29	0.69	6.60	2.32	4.48	1.08
$\mathbf{L_S}$ (nm)	1798	52	1603	165	1831	117	1376	262	2030	174
$\mathbf{L_A}$ (nm)	1554	53	1399	156	1391	60	1211	274	1522	110
$\mathbf{L_I}$ (nm)	244	41	204	49	441	105	165	37	507	114
$\mathbf{R_{IA}}$	0.16	0.03	0.15	0.04	0.32	0.08	0.15	0.06	0.33	0.07
$\mathbf{W_H}$ (nm)	869	453	578	270	732	265	420	155	417	161
$\mathbf{W_{Max}}$ (nm)	935	461	598	272	752	265	451	158	437	166
surface (μm^2)	335	147	468	190	2540	321	2208	1477	1463	619
%M (%)	47.97	2.12	61.08	4.38	41.24	4.66	43.08	5.50	41.78	4.20
DM (nm)	524	74	637	143	381	26	408	63	283	98
R (nm)	1129	441	965	362	1620	988	3937	2053	3369	2002
C (%)	1.98	1.16	0.30	0.41	0.00	0.00	0.00	0.00	0.16	0.36
$\mathbf{m_R}$ (nm^{-2})	$5.56\ 10^{-7}$	$3.37\ 10^{-7}$	$5.23\ 10^{-7}$	$1.82\ 10^{-7}$	$2.99\ 10^{-7}$	$1.58\ 10^{-7}$	$1.68\ 10^{-7}$	$7.97\ 10^{-8}$	$5.03\ 10^{-8}$	$5.57\ 10^{-8}$
$\mathbf{m_M}$ (nm^{-2})	$2.85\ 10^{-8}$	$2.22\ 10^{-8}$	$3.05\ 10^{-9}$	$2.69\ 10^{-9}$	$2.26\ 10^{-10}$	$2.09\ 10^{-10}$	$4.55\ 10^{-11}$	$1.02\ 10^{-10}$	$8.45\ 10^{-10}$	$1.30\ 10^{-9}$
$\mathbf{m_T}$ (nm^{-2})	$5.84\ 10^{-7}$	$3.44\ 10^{-7}$	$5.26\ 10^{-7}$	$1.82\ 10^{-7}$	$3.00\ 10^{-7}$	$1.58\ 10^{-7}$	$1.68\ 10^{-7}$	$7.97\ 10^{-8}$	$5.11\ 10^{-8}$	$5.60\ 10^{-8}$

Mitochondria are found throughout the cell but are mainly concentrated along the subsarcolemmal ring, where they are from 19 to more than 1000 times more numerous than in the other parts of the cell (Table 2). Depending on the species, the number of mitochondria in the subsarcolemmal ring varied from $7.31\ 10^{-8}$ to $1.12\ 10^{-7}$ mitochondria per nm^{-2}. Although their number seems to be more important in both basal species, *C. mento* and *P. denticulata* (Fig. 4), this assertion is globally not statistically supported. It remains that more important differences in $\mathbf{m_T}$ can be found between both basal species and *Pygocentrus cariba* (Kruskal-Wallis: $\chi^2 = 27.94$, df = 8, $P = 0.0005$; Dunn: Z = −3.52 and 3.57, $P = 0.005$ and 0.006), between *S. compressus* and *P. denticulata* (Dunn: Z = −2.76, $P = 0.03$) and between *S. spilopleura* and *P. cariba* (Dunn: Z = −3.57, $P = 0.01$). The combination of these first features (**size** and $\mathbf{m_T}$) indicated that the sonic muscle cells of *C. mento* and *P. denticulata* were small with a higher number of mitochondria in the subsarcolemmal space.

All the species except *P. cariba*, *P. nattereri* and *S. elongatus* had a central core. *Catoprion mento* proportionally had the highest ratio of core zone compared to the size of the cells (**C**) (1.98 ± 1.16, Table 2). Moreover, the ratio is statistically higher than in all other *Pygocentrus* species (Kruskal-Wallis: χ^2 =23.34, df = 8, *P* = 0.003; Dunn: Z = 2.93, 3.50 and 3.50, *P* = 0.04, 0.008 and 0.02), *S. elongatus* and *S. spilopleura* (Dunn: Z = 2.65 and 2.78, *P* = 0.04 and 0.048 respectively). Other quantitative features (e.g., **Ls** and **DM**) describing the sound-producing muscles of *C. mento* and *P. denticulata* are in the same range as those obtained in the studied *Serralsamus* and *Pygocentrus* species (Fig. 5). When considering all the features measured on transversal sections together, clustering methods separated two groups. The first group contained all the cells from *Catoprion mento*, *Pygopristis denticulata*, *Serrasalmus manueli* and 20% of the cells from *Pygocentrus nattereri*, while the second group contained all the cells from *Serrasalmus elongatus*, *S. compressus*, *S. spilopleura*, *Pygocentrus piraya*, *P. cariba* and 80% of the cells from *P. nattereri*. The interpretation of the PC1 on the sonic muscles shows the same division. The difference of PC1 is statistically supported between *Catoprion mento* and three other species: *S. compressus*, *P. cariba* and *P. nattereri* (Kruskal-Wallis: χ^2 = 29.93, df = 8, *P* = 0.00022; Dunn: Z = −3.06, −3.27 and −3.13, all *P* = 0.013. The same results are only observed for *Pygopristis denticulata* (Dunn: Z = 3.23, 3.44 and 3.30, *P* = 0.011, 0.021 and 0.017) and *S. manueli* (Dunn: Z = 2.64, −2.80 and −2.67, *P* = 0.033, 0.026 and 0.034).

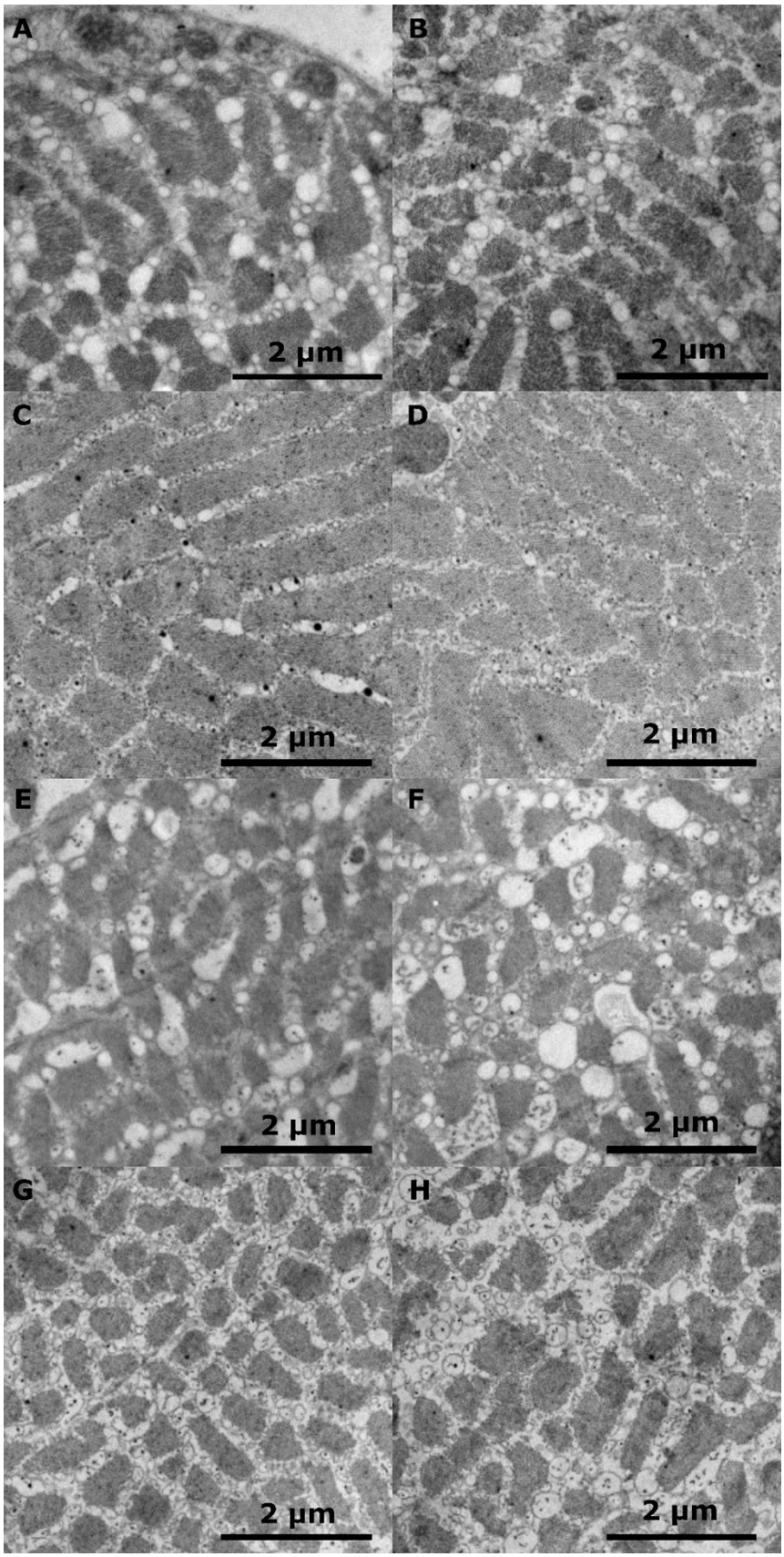

Fig. 5 Ultrastructure of sonic muscles (transversal sections). **A** and **B** *Catoprion mento*, **C** & **D** *Pygopristis denticulata*, **E** & **F** *Serrasalmus spilopleura* and **G** & **H** *Pygocentrus piraya*. Each picture is taken from a different cell.

In the genus *Serrasalmus*, the importance of the features varied depending on the species. For example, *S. manueli* muscle had a high **DM** (638 ± 122 nm); *S. spilopleura* muscle had a high **L**$_{\mathbf{S}}$ and **size** (2081 ± 212 nm and 2033 ± 460 µm^2 respectively); and *S. compressus* muscle had a low **%M** (32.78 ± 3.20%). **W**$_{\mathbf{H}}$ values statistically differed between *S. manueli* and the two species *S. elongatus* and *S. spilopleura* (Kruskal-Wallis: χ^2 =168.68, df = 8, P < 0.0001; Dunn: Z = 2.61 and −3.40, P = 0.02 and 0.001 respectively). **L**$_{\mathbf{S}}$ values of *S. spilopleura* statistically differed from those of the three other species of *Serrasalmus* (Kruskal-Wallis: χ^2 = 346.15, df = 8, P < 0.0001; Dunn: Z = −8.80, −8.77 and −10.40; all P < 0.0001) while these three species had similar values of **L**$_{\mathbf{S}}$ (Dunn: Z = −0.02, 1.60 and 1.63; P = 0.98, 0.13 and 0.13). In contrast, the differences of **R** were not statistically supported (Kruskal-Wallis: χ^2 = 21.34, df = 8, P = 0.006; Dunn: Z = −0.34, 1.75, 1.68, 1.16, 1.22 and −0.65; P = 0.83, 0.24, 0.23, 0.42, 0.40 and 0.66). *Serrasalmus compressus* muscle differed from *S. manueli* muscle for **%M** and **DM** (Kruskal-Wallis: χ^2 =26.47 and 32.79, df = 8, P = 0.0009 and < 0.0001; Dunn: Z = −3.48 and −3.76; P = 0.009 and 0.003 respectively) and from *S. spilopleura* for **m**$_{\mathbf{T}}$, **L**$_{\mathbf{S}}$ and **W**$_{\mathbf{H}}$ (Kruskal-Wallis: χ^2 = 27.94, 346.15 and 168.68; df = 8, P = 0.0005, < 0.0001 and < 0.0001; Dunn: Z = −2.81, −8.80 and −2.28; P = 0.04, < 0.0001 and 0.04 respectively) while this was not the case with *S. elongatus* (Dunn: all P > 0.05).

In *Pygocentrus spp.*, **L**$_{\mathbf{S}}$ was statistically different in the three species (Kruskal-Wallis: χ^2 = 346.15, df = 8, P < 0.0001; Dunn: Z = −9.22, 3.50 and 12.72; P < 0.0001, < 0.0001 and 0.0006). In addition, **HW** of sonic muscles of *P. piraya* was different from the two other species (Kruskal-Wallis: χ^2 = 168.68, df = 8, P < 0.0001; Dunn: Z = −6.53 and −6.46; both P < 0.0001).

Discussion

Sonic muscles vs. *epaxial muscles*

In the late 1970s, Eichelberg studied the fine structure of sonic muscles of an unnamed species of vocal piranha (Eichelberg, 1977). She described a higher abundance of sarcoplasmic reticulum, triads positioned at the level of the Z lines but having a considerably smaller central vesicle and a high abundance of mitochondria at the fibre periphery (Eichelberg, 1977). In our study on numerous different species, we confirm that this former description can be applied to all vocal taxa from the family, regardless of the fine mechanism. In comparison to the white epaxial muscles, fibres of the sound producing muscles are thinner with a smaller diameter, possess a smaller ratio of space devoted to myofibrils and a thicker subsarcolemmal ring having more mitochondria per surface unit than fibres of epaxial muscles. Inside myofibrils,

sarcomeres are longer and thinner than in the epaxial muscles and their number per surface unit is higher.

Sonic muscles of the different species

The evolutionary history hypothesis of sound production in piranhas can be explained in a few steps. Some intercostal muscle fibres were first used to produce isolated pulsed sounds in herbivorous species (Mélotte et al., 2019). Modifications at the level of these intercostal muscle fibres have led to the two kinds of mechanisms that can be observed in the monotypic genera *Pygopristis* and *Catoprion* (Mélotte et al., 2019). In both species, right and left muscles are not physically connected. In the more derived species (*Serrasalmus* and *Pygocentrus*), the left and right sonic muscles possess a vertical orientation and are both connected ventrally by a common tendon mechanism (Mélotte et al., 2019; Nelson, 1961). This latter kind of mechanism is the most abundant since *Serrasalmus* and *Pygocentrus* respectively possess 31 and 3 species (or 4 if *P. palometa* is included) (Fricke, Eschmeyer, & Van der Laan, 2021). However, this mechanism appears well conserved within both taxa (Mélotte et al., 2016). All these modifications to the sonic apparatus are coupled with an increase in the innervation network, muscle thickening and sound complexity. Taxa having these mechanisms are associated with a higher speciation rate than other vocal piranha species, however, the relation between the diversification process and the sound producing abilities is not clear.

All three kinds of sonic apparatus are based on the use of high-speed sonic muscles. Despite caution due to the small sample size, the main result of this study can be found in the modifications of the muscle ultrastructure. Figure 6 shows that the transition from white epaxial to sound-producing muscles (**DM**, **R** and **%M** are correlated with PC1, $\rho = -0.95$, 0.85 and -0.90 respectively, all adjusted *P*-values < 0.001) has different degrees of specialization (Fig. 6). Interestingly, the species with the most primitive mechanisms, *Pygopristis* and *Catoprion* have a pivotal position in the modification scheme. In *P. denticulata*, it is quite interesting to note that sonic muscles possess the insertion structure of costal muscles but the ultrastructure of a classic sonic muscle, reinforcing the hypothesis of the hypaxial origin (Banse et al., 2021; Mélotte et al., 2019; Millot & Parmentier, 2014). The PCA analysis also shows that its organization is closer to epaxial muscle characteristics. In comparison to other species, the sonic muscle of *P. denticulata* still possesses a combination of features (high ratio of space devoted to myofibrils, a small subsarcolemmal ring; Table 2, Fig. 5), that could place it between the ultrastructure found in epaxial muscles and sonic muscles of other species. All these features indicate that the ability to achieve fast contraction to produce sustained sounds appeared early

in the evolutionary history of the taxa. From a functional point of view, the forced vibration of the swim bladder in this species implies the requirement of force to move the ribs and the fascia joining the first rib to the vertebral column. In *Serrasalmus* and *Pygocentrus* species, the muscles are acting directly on the swim bladder and the lack of intermediate structures means that less force is required to vibrate the swim bladder. This functional difference fully implies that more numerous myofibrils are required in *P. denticulata* since the ratio of myofibrils/sarcoplasmic reticulum is related to the ability to develop force or speed (Parmentier et al., 2021; L. C. Rome et al., 1999; Lawrence C. Rome & Lindstedt, 1998). The primitive state of the system could also be related to the fact that all the studied vocal species except *P. denticulata* are able to make sounds when the fish is hand-held underwater by researchers (Mélotte et al., 2019).

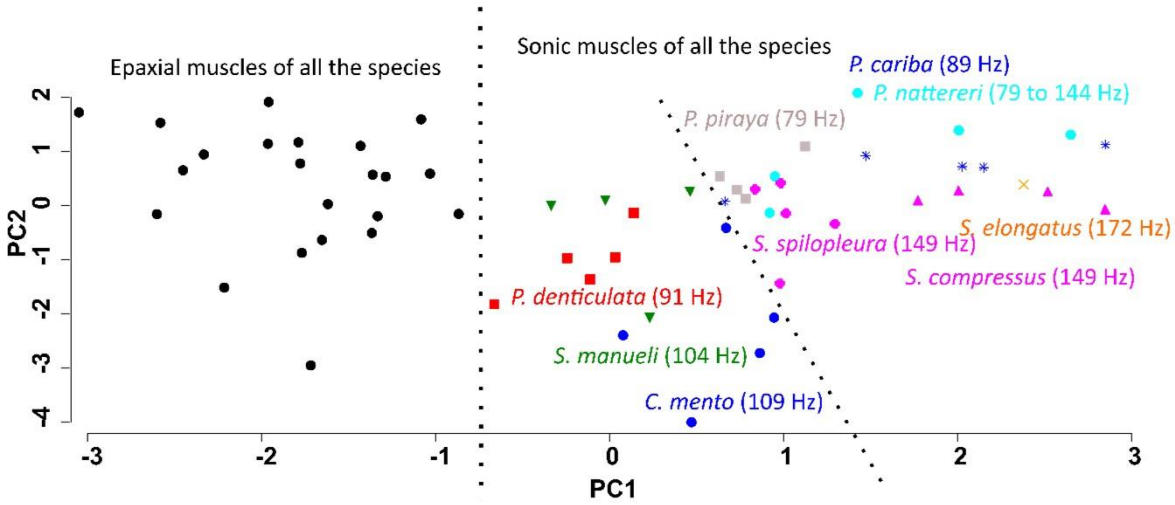

Fig. 6 Scores of the principal component analysis on the features measured on transversal sections for all epaxial and sonic muscles. ● = Epaxial muscles of all the species, ■ = Sonic muscles of *Pygopristis denticulata*, ● = Sonic muscles of *Catoprion mento*, ▼ = Sonic muscles of *Serrasalmus manueli*, ● = Sonic muscles of *Serrasalmus spilopleura*, ▲= Sonic muscles of *Serrasalmus compressus*, X = Sonic muscles of *Serrasalmus elongatus*, ■ = Sonic muscles of *Pygocentrus piraya*, ∗ = Sonic muscles of *Pygocentrus cariba* and ● = Sonic muscles of *Pygocentrus nattereri*. The fundamental frequency of the sounds produced by each species are from Mélotte et al. 2016, Mélotte et al. 2019 and Raick et al. 2020. The dashed lines illustrate the three groups observed, from left to right, (1) epaxial muscles of all the species, (2) sonic muscles of basal species and *S. manueli* and (3) sonic muscles of all the *Pygocentrus* species and all the other *Serrasalmus* species. Importance of components: 41.3% and 25.2% respectively. **DM**, **R** and **%M** are correlated with PC1, $\rho = -0.95$, 0.85 and −0.90 respectively, all adjusted *P*-values < 0.001.

According to the muscle ultrastructure, the sonic muscle of *Catoprion mento* could also be placed in an intermediate position since it shows features situated between *Pygopristis denticulata* and the majority of *Pygocentrus* and *Serrasalmus* species.

When considering *Serrasalmus* species, it is interesting to note that there is heterogeneity in the muscle features. The sonic apparatus appears to be well conserved but minor modifications of (at least) the sonic muscle ultrastructure should favour differences in the acoustic abilities, such as sound duration or pulse period and the related frequency. For example, *S. manueli*, the species that possesses a smaller ratio of space devoted to sarcoplasmic reticulum, is also the *Serrasalmus* species that has longer cycle periods corresponding to a lower fundamental frequency, 104 Hz (Mélotte et al., 2016). In contrast, *S. elongatus* had higher PC1 values (i.e. low **DM** and **%M**, and high **R** values) and is able to sustain frequencies around 172 Hz (Mélotte et al., 2016). Similar observations could be realized in the *Pygocentrus* genus. Relationships between histological ultrastructure and acoustic features correspond to previous studies showing that, at least, a low ratio of myofibrils and a high mitochondria content are required for fast and sustained contractions (Fine, Bernard, & Harris, 1993; Friedrich Ladich, 2001).

Acknowledgements

The authors thank Marc Thiry for his advice, Sarah Smeets for her technical assistance with fixation and staining, and Erica Marucco for interesting discussions on the subject.

Funding

This work was supported by the FRS-FNRS (PDR no. 23625340).

Author contributions

EP & XR designed and supervised the study. EP and XR collected the biological material. XR, NT and PC realized the observations. XR analysed the data. XR wrote the first version of the manuscript. XR & EP wrote the final version with input from NT and PC.

Competing interests

The authors declare no competing interests.

Data Availability Statement

The data that support the findings of this study are available on request from the corresponding author (XR).

Bibliography

Appelt, D., Shen, V., & Franzini-Armstrong, C. (1991). Quantitation of Ca ATPase, feet and mitochondria in superfast muscle fibres from the toadfish, *Opsanus tau*. *Journal of Muscle Research and Cell Motility*, *12*, 543–552.

Banse, M., Chagnaud, B. P., Huby, A., Parmentier, E., & Kéver, L. (2021). Sound production in piranhas is associated with modifications of the spinal locomotor pattern. *Journal of Experimental Biology*, *224*. https://doi.org/10.1242/jeb.242336

Bass, A. H., Gilland, E. H., & Baker, R. (2008). Evolutionary Origins for Social Vocalization in a Vertebrate Hindbrain-Spinal Compartment. *Science*, *321*, 417–421.

Boyle, K. S., Riepe, S., Bolen, G., & Parmentier, E. (2015). Variation in swim bladder drumming sounds from three doradid catfish species with similar sonic morphologies. *The Journal of Experimental Biology*, *218*, 2881–2891.

Eichelberg, H. (1977). Fine structure of the drum muscles of piranha (Serrasalminae, Characidae). *Cell and Tissue Research*, *185*, 547–555.

Eichelberg, H. (1978). Local degenerative changes in the drum muscles of piranhas (Serrasalminae, Characidae). *Cell and Tissue Research*, *188*, 75–82.

Fine, M. L., Bernard, B., & Harris, T. M. (1993). Functional morphology of toadfish sonic muscle fibers: relationship to possible fiber division. *Canadian Journal of Zoology*, *71*, 2262–2274.

Fricke, R., Eschmeyer, W. N., & Van der Laan, R. (2021). Eschmeyer's catalog of fishes: genera, species, references. Retrieved June 10, 2021, from http://researcharchive.calacademy.org/research/ichthyology/catalog/fishcatmain.asp

Kastberger, G. (1981). Economy of sound production in piranhas (Serrasalminae, Characidae): ll. Functional properties of sound emitter. *Zoologische Jahrbücher Physiologie*, *85*, 113–125.

Ladich, Friedrich. (2001). Sound-generating and -detecting motor system in catfish: Design of Swimbladder Muscles in Doradids and Pimelodids. *The Anatomical Record*, *263*, 297–306.

Ladich, Friedrich, & Bass, A. H. (2005). Sonic Motor Pathways in Piranhas with a Reassessment of Phylogenetic Patterns of Sonic Mechanisms among Teleosts. *Brain,*

Behavior and Evolution, *66*, 167–176.

Markl, H. (1971). Schallerzeugung bei Piranhas (Serrasalminae, Characidae). *Zeitschrift Für Vergleichende Physiologie*, *74*, 39–56.

Mélotte, G., Raick, X., Vigouroux, R., & Parmentier, E. (2019). Origin and evolution of sound production in Serrasalmidae. *Biological Journal of the Linnean Society*, *128*, 403–414.

Mélotte, G., Vigouroux, R., Michel, C., & Parmentier, E. (2016). Interspecific variation of warning calls in piranhas: a comparative analysis. *Scientific Reports*, *6*, 36127.

Millot, S., & Parmentier, E. (2014). Development of the ultrastructure of sonic muscles: a kind of neoteny? *BMC Evolutionary Biology*, *14*, 24.

Millot, S., Vandewalle, P., & Parmentier, E. (2011). Sound production in red-bellied piranhas (*Pygocentrus nattereri*, Kner): an acoustical, behavioural and morphofunctional study. *Journal of Experimental Biology*, *214*, 3613–3618.

Nelson, E. M. (1961). The swim bladder in the Serrasalminae, with notes on additional morphological features. *Feldania Zoology*, *39*, 603–624.

Parmentier, E., Bouillac, G., Dragicevic, B., Dulcic, J., & Fine, M. (2010). Call properties and morphology of the sound-producing organ in *Ophidion rochei* (Ophidiidae). *Journal of Experimental Biology*, *213*, 3230–3236.

Parmentier, E., & Diogo, R. (2006). Evolutionary trends of swimbladder sound mechanisms in some teleost fishes. In F Ladich, S. P. Collin, P. Moller, & B. G. Kapoor (Eds.), *Communication in fishes, vol 1* (pp. 45–70). Enfield: Science Publisher Inc.

Parmentier, E., Marucco Fuentes, E., Millot, M., Raick, X., & Thiry, M. (2021). Sound production, hearing sensitivity, and in-depth study of the sound-producing muscles in the cowfish (*Lactoria cornuta*). *Journal of Anatomy*, *238*, 956–969.

Raick, X., Huby, A., Kurchevski, G., Godinho, A. L., & Parmentier, É. (2020a). Use of bioacoustics in species identification: piranhas from genus *Pygocentrus* (Teleostei: Serrasalmidae) as a case study. *PLoS ONE*, *15*, e0241316.

Raick, X., Huby, A., Kurchevski, G., Godinho, A. L., & Parmentier, É. (2020b). Yellow-eyed piranhas produce louder sounds than red-eyed piranhas in an invasive population of *Serrasalmus marginatus*. *Journal of Fish Biology*, *97*, 1676–1680.

Raick, X., Rountree, R., Kurchevski, G., Juanes, F., Huby, A., Godinho, A. L., & Parmentier, É. (2021). Acoustic homogeneity in the piranha *Serrasalmus maculatus*. *Journal of Fish Biology*, jfb.14662.

Rome, L. C., Cook, C., Syme, D. A., Connaughton, M. A., Ashley-Ross, M., Klimov, A., … Goldman, Y. E. (1999). Trading force for speed: Why superfast crossbridge kinetics leads to superlow forces. *Proceedings of the National Academy of Sciences*, *96*, 5826–5831.

Rome, L. C., Syme, D. A., Hollingworth, S., Lindstedt, S. L., & Baylor, S. M. (1996). The whistle and the rattle: the design of sound producing muscles. *Proceedings of the National Academy of Sciences*, *93*, 8095–8100.

Rome, Lawrence C., & Lindstedt, S. L. (1998). The Quest for Speed: Muscles Built for High-Frequency Contractions. *Physiology*, *13*, 261–268.